

This article was downloaded by:

On: 23 January 2011

Access details: *Access Details: Free Access*

Publisher *Taylor & Francis*

Informa Ltd Registered in England and Wales Registered Number: 1072954 Registered office: Mortimer House, 37-41 Mortimer Street, London W1T 3JH, UK



## Journal of Coordination Chemistry

Publication details, including instructions for authors and subscription information:

<http://www.informaworld.com/smpp/title~content=t713455674>

### Ruthenium(II) complexes of 2-(2'-pyridyl)naphthoimidazole: synthesis, characterization and DNA-binding studies

Yun-Jun Liu<sup>a</sup>; Wen-Jie Mei<sup>a</sup>; Jia-Zheng Lu<sup>a</sup>; Hao-Jie Zhao<sup>a</sup>; Li-Xin He<sup>a</sup>; Fu-Hai Wu<sup>b</sup>

<sup>a</sup> School of Pharmacy, Guangdong Pharmaceutical University, Guangzhou, 510006, P.R. China <sup>b</sup> School of Public Health, Guangdong Pharmaceutical University, Guangzhou, 510006, P.R. China

**To cite this Article** Liu, Yun-Jun , Mei, Wen-Jie , Lu, Jia-Zheng , Zhao, Hao-Jie , He, Li-Xin and Wu, Fu-Hai(2008) 'Ruthenium(II) complexes of 2-(2'-pyridyl)naphthoimidazole: synthesis, characterization and DNA-binding studies', *Journal of Coordination Chemistry*, 61: 20, 3213 – 3224

**To link to this Article:** DOI: 10.1080/00958970802017653

**URL:** <http://dx.doi.org/10.1080/00958970802017653>

PLEASE SCROLL DOWN FOR ARTICLE

Full terms and conditions of use: <http://www.informaworld.com/terms-and-conditions-of-access.pdf>

This article may be used for research, teaching and private study purposes. Any substantial or systematic reproduction, re-distribution, re-selling, loan or sub-licensing, systematic supply or distribution in any form to anyone is expressly forbidden.

The publisher does not give any warranty express or implied or make any representation that the contents will be complete or accurate or up to date. The accuracy of any instructions, formulae and drug doses should be independently verified with primary sources. The publisher shall not be liable for any loss, actions, claims, proceedings, demand or costs or damages whatsoever or howsoever caused arising directly or indirectly in connection with or arising out of the use of this material.

## Ruthenium(II) complexes of 2-(2'-pyridyl)naphthoimidazole: synthesis, characterization and DNA-binding studies

YUN-JUN LIU\*†, WEN-JIE MEI†, JIA-ZHENG LU†, HAO-JIE ZHAO†,  
LI-XIN HE† and FU-HAI WU‡

†School of Pharmacy, Guangdong Pharmaceutical University, Guangzhou, 510006,  
P.R. China

‡School of Public Health, Guangdong Pharmaceutical University, Guangzhou, 510006,  
P.R. China

(Received 23 September 2007; in final form 17 December 2007)

The perchlorate salts of two new ruthenium(II) complexes incorporating 2-(2'-pyridyl)naphthoimidazole are synthesized in good yield. Complexes  $[\text{Ru}(\text{phen})_2(\text{PYNI})]^{2+}$  (phen = 1,10-phenanthroline) **1** and  $[\text{Ru}(\text{dmp})_2(\text{PYNI})]^{2+}$  (dmp = 2,9-dimethyl-1,10-phenanthroline, PYNI = 2-(2'-pyridyl)naphthoimidazole) **2** are fully characterized by elemental analysis, FAB-MS, ES-MS,  $^1\text{H}$  NMR and cyclic voltammetric methods. The DNA-binding behavior of the complexes have been studied by spectroscopic titration, viscosity measurements and thermal denaturation. Absorption titration and thermal denaturation studies reveal that these complexes are moderately strong binders of calf-thymus DNA (CT-DNA), with their binding constants spanning the range  $(2.73\text{--}5.35) \times 10^4 \text{ M}^{-1}$ . The experimental results show that **1** interacts with calf thymus DNA (CT-DNA) by intercalative mode, while **2** binds to CT-DNA by partial intercalation.

*Keywords:* Ruthenium(II) complex; DNA; Thermal denaturation

### 1. Introduction

Over the past decade, DNA-binding metal complexes have been extensively studied as DNA structural probes, DNA-dependent electron transfer and sequence-specific cleaving agents and potential anticancer drugs [1–3]. The interaction of Ru(II) polypyridyl complexes with DNA has attracted considerable interest. An understanding of how molecules bind to DNA will be potentially useful in the design of new drugs and highly sensitive spectroscopic and reactive probes and diagnostic reagents [1, 4–6]. The most interesting complexes are Ru(II) complexes containing dipyridophenazine (dppz) [7–25], such as  $[\text{Ru}(\text{bpy})_2(\text{dppz})]^{2+}$  (bpy = 2,2'-bipyridine) and  $[\text{Ru}(\text{phen})_2(\text{dppz})]^{2+}$  (phen = 1,10-phenanthroline). Although lacking luminescence in aqueous solution, they show intense luminescence in the presence of DNA, termed as the “light switch” for DNA [7–10]. The luminescence enhancement was proposed to be protection of the

\*Corresponding author. Email: lyjche@163.com

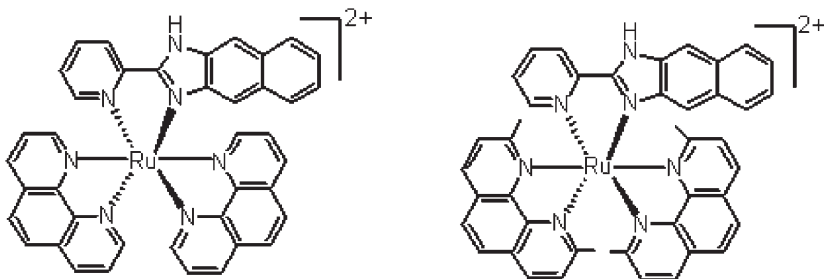
phenazine nitrogen atoms from solvent water when the dppz ligand intercalated between the base pairs of DNA.

Upon binding to DNA, the small molecules are stabilized through a series of weak interactions such as  $\pi$ -stacking interactions of aromatic heterocyclic groups between the base pairs (intercalation), hydrogen-bonding and van der Waals interactions of functional groups bound along the groove of the DNA helix [26]. Many applications require that complexes bind to DNA through an intercalative mode. Therefore much work has been done on modifying the intercalative ligand; the influence of the ancillary ligands of the complexes on DNA-binding has received little attention. Since the octahedral polypyridyl Ru(II) complexes bind to DNA in three dimensions, the ancillary ligands can also play an important role in governing DNA-binding of these complexes. So it is important to find the effects of ancillary ligands on binding to DNA. To more clearly study the effects of ancillary ligands on DNA-binding behavior of Ru(II) complexes, the selection of intercalative ligand is also very important. An appropriate intercalative ligand is helpful to distinguish the small differences of interaction of the complexes containing different ancillary ligands with DNA. In this article, two new Ru(II) polypyridyl complexes  $[\text{Ru}(\text{phen})_2(\text{PYNI})]^{2+}$  **1** (phen = 1,10-phenanthroline) and  $[\text{Ru}(\text{dmp})_2(\text{PYNI})]^{2+}$  **2** (dmp = 2,9-dimethyl-1,10-phenanthroline, PYNI = 2-(2'-pyridyl)naphthoimidazole, scheme 1) have been synthesized and characterized by elemental analysis, FAB-MS, ES-MS,  $^1\text{H}$  NMR and cyclic voltammetry. Their DNA-binding behaviors were investigated by absorption titration, luminescence spectroscopy, viscosity measurements and thermal denaturation.

## 2. Experimental

### 2.1. Materials and method

Calf thymus DNA (CT-DNA) was obtained from the Sino-American Biotechnology Company. Doubly-distilled water was used to prepare buffers (5 mM tris(hydroxymethylaminomethane)-HCl, 50 mM NaCl, pH = 7.2). A solution of calf thymus DNA in the buffer gave a ratio of UV absorbance at 260 and 280 nm of ca. 1.8–1.9:1, indicating that the DNA was sufficiently free of protein [27]. The DNA concentration per nucleotide was determined by absorption spectroscopy using the molar absorption coefficient ( $6600 \text{ M}^{-1} \text{ cm}^{-1}$ ) at 260 nm [28].



Scheme 1. Structures of  $[\text{Ru}(\text{phen})_2(\text{PYNI})]^{2+}$  and  $[\text{Ru}(\text{dmp})_2(\text{PYNI})]^{2+}$ .

## 2.2. Physical measurements

Microanalysis (C, H, and N) was carried out with a Perkin-Elmer 240Q elemental analyzer. Fast atom bombardment (FAB) mass spectra were recorded on a VG ZAB-MS spectrometer in a 3-nitrobenzyl alcohol matrix. Electrospray mass spectra (ES-MS) were recorded on a LCQ system (Finnigan MAT, USA) using methanol as mobile phase. The spray voltage, tube lens offset, capillary voltage and capillary temperature were set at 4.50 KV, 30.00 V, 23.00 V and 200°C, respectively, and the quoted  $m/z$  values are for the major peaks in the isotope distribution.  $^1\text{H}$  NMR spectra were recorded on a Varian-500 spectrometer. All chemical shifts were given relative to tetramethylsilane (TMS). UV-Vis spectra were recorded on a Shimadzu UV-3101PC spectrophotometer at room temperature.

Cyclic voltammetric measurements were performed on a CHI 660A Electrochemical Workstation. All samples were purged with nitrogen prior to measurements. A standard three-electrode system comprising of platinum microcylinder working electrode, platinum-wire auxiliary electrode and a saturated calomel reference electrode (SCE) was used.

## 2.3. DNA-binding studies

The absorption titrations of ruthenium(II) complex in buffer were performed by using a fixed ruthenium complex concentration (20  $\mu\text{M}$ ) to which the DNA stock solution was added. Ruthenium-DNA solutions were allowed to incubate for 5 min before the absorption spectra were recorded. In order to further illustrate the binding strength of the complex, the intrinsic binding constant  $K$  with CT-DNA was obtained by monitoring the change in the absorbance at metal-to-ligand transfer (MLCT), with increasing concentration of DNA. The following equation was applied [29]:

$$\frac{[\text{DNA}]}{\varepsilon_a - \varepsilon_f} = \frac{[\text{DNA}]}{\varepsilon_b - \varepsilon_f} + \frac{1}{K_b(\varepsilon_b - \varepsilon_f)} \quad (1)$$

where  $[\text{DNA}]$  is the concentration of DNA in base pairs,  $\varepsilon_a$ ,  $\varepsilon_f$  and  $\varepsilon_b$  correspond to the apparent absorption coefficients  $A_{\text{obsd}}/[\text{Ru}]$ , the extinction coefficient for the free ruthenium complex and the extinction coefficient for the ruthenium complex in the fully bound form, respectively. In plots of  $[\text{DNA}]/(\varepsilon_a - \varepsilon_f)$  versus  $[\text{DNA}]$ ,  $K_b$  is given by the ratio of slope to the intercept.

For the steady-state emission quenching experiment using  $[\text{Fe}(\text{CN})_6]^{4-}$  as quencher, according to the classical Stern-Volmer equation (2) [30]

$$I_0/I = 1 + Kr \quad (2)$$

where  $I_0$  and  $I$  are the luminescence intensities in the absence and presence of  $[\text{Fe}(\text{CN})_6]^{4-}$ , respectively.  $K$  is a linear Stern-Volmer quenching constant dependent on the ratio of the bound concentration of Ru(II) complex to the concentration of DNA;  $r$  is the concentration of the quencher  $[\text{Fe}(\text{CN})_6]^{4-}$ . In the plot of  $I_0/I$  versus  $r$ , the Stern-Volmer quenching constant  $K$  is given by the slope.

Viscosity measurements were carried out using an Ubbelodhe viscometer maintained at 28.0 ( $\pm 0.1$ )°C in a thermostatic bath. DNA samples approximately 200 base pairs in average length were prepared by sonicating in order to minimize

complexities arising from DNA flexibility [31]. Flow time was measured with a digital stopwatch, and each sample was measured three times, and an average flow time was calculated. Data were presented as  $(\eta/\eta_0)^{1/3}$  versus binding ratio [32], where  $\eta$  is the viscosity of DNA in the presence of complex and  $\eta_0$  is the viscosity of DNA alone.

Thermal denaturation studies were carried out with a Perkin-Elmer Lambda 35 spectrophotometer equipped with a Peltier temperature-controlling programmer ( $\pm 0.1^\circ\text{C}$ ). The melting curves were obtained by measuring the absorbance at 260 nm for solutions of CT-DNA (100  $\mu\text{M}$ ) in the absence and presence of Ru(II) complexes. The temperature was scanned from 50 to  $90^\circ\text{C}$  at a speed of  $1^\circ\text{C min}^{-1}$ . The melting temperature ( $T_m$ ) was taken as the mid-point of the hyperchromic transition.

#### 2.4. Synthesis and characterization

*Cis*-[Ru(phen)<sub>2</sub>Cl<sub>2</sub>]·2H<sub>2</sub>O [33], *cis*-[Ru(dmp)<sub>2</sub>Cl<sub>2</sub>]·2H<sub>2</sub>O [34] and PYNI [35] were synthesized according to literature procedures.

**2.4.1. [Ru(phen)<sub>2</sub>(PYNI)](ClO<sub>4</sub>)<sub>2</sub> (1).** A mixture of *cis*-[Ru(phen)<sub>2</sub>Cl<sub>2</sub>]·2H<sub>2</sub>O (0.284 g, 0.5 mmol) and PYNI (0.123 g, 0.5 mmol) in ethylene glycol (20 cm<sup>3</sup>) was refluxed under argon for 6 h to give a clear red solution. Upon cooling, a brown red precipitate was obtained by dropwise addition of saturated aqueous NaClO<sub>4</sub> solution. The crude product was purified by column chromatography on neutral alumina with CH<sub>3</sub>CN-toluene (3:1, v/v) as eluant. The brown red band was collected, the solvent was removed under reduced pressure and a brown red powder was obtained. Yield: 66%. Anal. Found: C, 53.07; H, 3.04; N, 10.82. Calcd for C<sub>40</sub>H<sub>27</sub>N<sub>7</sub>Cl<sub>2</sub>O<sub>8</sub>Ru: C, 53.05; H, 3.00; N, 10.83%. <sup>1</sup>H NMR (ppm, DMSO-d<sub>6</sub>):  $\delta$ : 8.85 (d, 1H, J = 8.6 Hz), 8.71 (d, 2H, J = 8.5 Hz), 8.62 (d, 1H, J = 8.5 Hz), 8.50 (d, 1H, J = 8.4 Hz), 8.43 (d, 1H, J = 8.2 Hz), 8.36 (s, 4H), 8.26 (t, 1H, J = 7.5 Hz), 8.23 (d, 1H, J = 8.0 Hz), 8.0–8.04 (m, 2H), 7.86–7.90 (m, 2H), 7.80–7.85 (m, 3H), 7.74–7.79 (m, 2H), 7.57 (d, 1H, J = 7.8 Hz), 7.10 (t, 1H, J = 7.6 Hz), 7.03 (t, 1H, J = 7.5 Hz), 6.96 (d, 1H, J = 8.2 Hz), 5.45 (s, 1H). ES-MS (CH<sub>3</sub>OH): *m/z* 706.2 ([M–2ClO<sub>4</sub>–H]<sup>+</sup>), 354.6 ([M–2ClO<sub>4</sub>]<sup>2+</sup>).

**2.4.2. [Ru(dmp)<sub>2</sub>(PYNI)](ClO<sub>4</sub>)<sub>2</sub> (2).** This complex was synthesized with the same method described for **1**. Yield: 64%. Anal. Found: C, 54.96; H, 3.64; N, 10.23; Calcd for C<sub>44</sub>H<sub>35</sub>N<sub>7</sub>Cl<sub>2</sub>O<sub>8</sub>Ru: C, 54.95; H, 3.67; N, 10.19%; <sup>1</sup>H NMR (DMSO-d<sub>6</sub>, 500 MHz)  $\delta$ : 8.34 (d, 1H, J = 8.8 Hz), 8.23 (d, 1H, J = 8.5 Hz), 8.19 (d, 2H, J = 8.6 Hz), 8.03 (d, 1H, J = 8.5 Hz), 7.88 (t, 2H, J = 7.8 Hz), 7.75–7.79 (m, 2H), 7.67 (d, 1H, J = 8.8 Hz), 7.47 (d, 2H, J = 8.0 Hz), 7.45 (d, 2H, J = 8.2 Hz), 7.23 (t, 1H, J = 7.6 Hz), 7.12–7.17 (m, 2H), 7.05–7.09 (m, 2H), 7.03 (d, 1H, J = 8.4 Hz), 6.91–6.94 (m, 1H), 6.81 (d, 1H, J = 8.5 Hz), 5.00 (s, 1H), 2.30 (s, 6H), 2.01 (s, 6H). ES-MS (CH<sub>3</sub>OH): *m/z* 762.1 ([M–2ClO<sub>4</sub>–H]<sup>+</sup>), 381.7 ([M–2ClO<sub>4</sub>]<sup>2+</sup>).

**Caution!** Perchlorate salts of metal complexes with organic ligands are potentially explosive, and only small amounts of the material should be prepared and handled with great care.

### 3. Results and discussion

#### 3.1. Electrochemical studies

Electrochemical behaviors of  $[\text{Ru}(\text{phen})_2(\text{PYNI})]^{2+}$  and  $[\text{Ru}(\text{dmp})_2(\text{PYNI})]^{2+}$  have been studied in acetonitrile by cyclic voltammetry. Both complexes exhibit well-defined waves corresponding to the metal-based oxidation and successive ligand-based reduction in the sweep range from  $-2.0$  to  $2.0$  V (figure 1). This pattern is common to  $d^6$  metal polypyridyl complexes, where the redox orbitals are localized on the individual ligand [36]. The electrochemical data for **1** and **2** with  $[\text{Ru}(\text{phen})_3]^{2+}$  are listed in table 1. An oxidation wave corresponding to the  $\text{Ru}^{\text{III}}/\text{Ru}^{\text{II}}$  couple was observed at 1.43 and 1.37 V for **1** and **2** (versus SCE), respectively, near the value of  $[\text{Ru}(\text{phen})_3]^{2+}$  (1.40 V) [37]. By comparing with the redox behavior of  $[\text{Ru}(\text{bpy})_3]^{2+}$  and related complexes [38–40], the first reduction is assigned to reduction centered on the

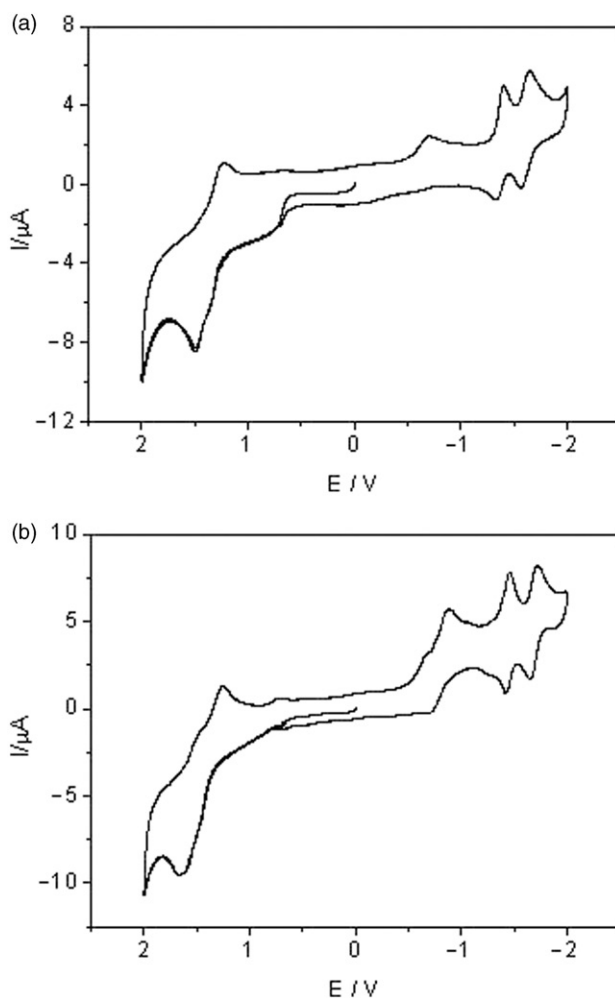


Figure 1. Cyclic voltammogram of **1**(a) and **2**(b) in MeCN.

Table 1. Electrochemical data of the ruthenium(II) complexes.

Complexes	$E_{1/2}$ (V) vs. SCE <sup>a</sup>			
	Ru <sup>II/III</sup>	Ligand reduction		
[Ru(phen) <sub>3</sub> ] <sup>2+</sup>	1.40	-1.41	-1.54	-1.84
[Ru(phen) <sub>2</sub> (PYNI)] <sup>2+</sup>	1.37	-0.66	-1.36	-1.59
[Ru(dmp) <sub>2</sub> (PYNI)] <sup>2+</sup>	1.43	-0.79	-1.44	-1.73

<sup>a</sup>All data were measured in 0.1 M NBu<sub>4</sub>ClO<sub>4</sub>-MeCN, error in potentials was  $\pm 0.02$  V; scan rate = 100 mV s<sup>-1</sup>.

intercalative ligand (PYNI) and the rest of the reductions are usually assigned the reductions centered on the ancillary ligands [36], characteristic of two phen or dmp ligands. The different values of reduction potentials arise from different intercalative or ancillary ligands (table 1). For **2**, the incorporation of the electron-releasing substituents (-CH<sub>3</sub> in phen) decrease the reduction potentials compared with **1**.

### 3.2. Absorption spectroscopic studies

The electronic absorption spectra of **1** and **2** mainly consist of two resolved bands. The high energy absorption at 320–350 nm is attributed to  $\pi \rightarrow \pi^*$ ; the band centered at 460–470 nm is assigned to metal-to-ligand charge transfer (MLCT) by comparison with the spectrum of other polypyridyl Ru(II) complexes [41–44].

Figure 2 shows electronic spectra of the two Ru(II) complexes titrated with calf thymus DNA (CT-DNA). With increasing concentration of CT-DNA, all absorption bands show clear hypochromism and red shift. The extent of hypochromism ( $H\%$ ), as defined by  $H\% = 100\% (A_{\text{free}} - A_{\text{bound}}) / A_{\text{free}}$  of the MLCT transition bands of **1** at 463 nm and **2** at 465 nm reach 26.5% and 19.8%, and bathochromism of **2** nm and **1** nm, respectively. Comparing the hypochromism of the two complexes with that of [Ru(phen)<sub>3</sub>]<sup>2+</sup> (hypochromism in MLCT band at 445 nm of 12% and red shift of 2 nm) [3], which interacts with DNA through a semi-intercalation or quasi-intercalation [45], these spectral characteristics obviously suggest that **1** and **2** interact with DNA most likely through a mode that involves a stacking interaction between the aromatic chromophore and the base pairs of DNA.

The intrinsic constants  $K$ , which illustrate the binding strength of the two complexes, were determined by monitoring the changes of absorbance in the MLCT band with increasing concentration of DNA. The intrinsic binding constants  $K$  of **1** and **2** were derived as  $5.35 \times 10^4 \text{ M}^{-1}$  and  $2.73 \times 10^4 \text{ M}^{-1}$ , respectively. These values are similar to that of [Ru(L)<sub>2</sub>(PMIP)]<sup>2+</sup> [L = bpy ( $2.03 \times 10^4$ ), phen ( $5.70 \times 10^4$ ) and dmp ( $1.17 \times 10^4$ )] [46], but smaller than that observed for [Ru(bpy)<sub>2</sub>(dppz)]<sup>2+</sup> ( $> 10^6$ ) [47]. The difference between the two intrinsic constants of these complexes with CT-DNA arises from different ancillary ligand. Complex **2** shows the least binding strength to double-helical DNA. Substitution on the 2- and 9-positions of the ancillary phen ligands may cause severe steric constraints near the core of Ru<sup>II</sup> when the complex intercalates into the DNA base pairs. The methyl groups may come into close proximity with base pairs at the intercalation sites. These steric clashes then prevent the complex from intercalating effectively, which causes a diminution of the intrinsic constant. Such clashes would not be present without substitution of the ancillary phen ligands [40].

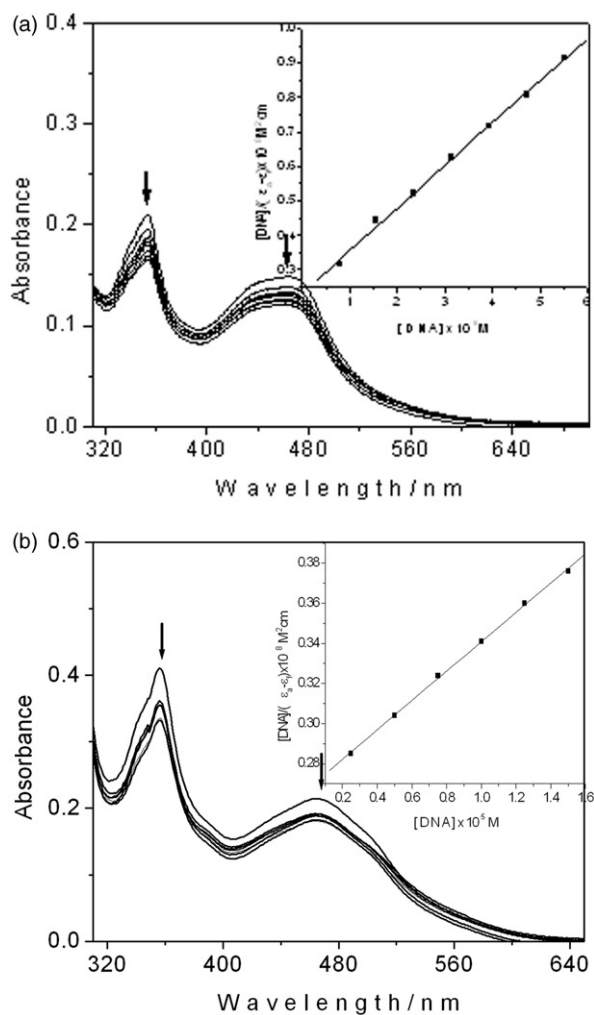


Figure 2. Absorption spectra in *Tris*-HCl buffer upon addition of CT- DNA in the presence of **1**(a) and **2**(b).  $[\text{Ru}] = 20 \mu\text{M}$ . Arrow shows the absorbance changing upon increase of DNA concentration. Inset: plots of  $[\text{DNA}] / (\epsilon_d - \epsilon_f)$  vs.  $[\text{DNA}]$  for the titration of DNA with Ru(II) complex.

The results show that the DNA binding affinities of these complexes closely correlate to the effects of ancillary ligands.

### 3.3. Luminescence spectroscopic study

Figure 3 shows that fixed amounts ( $5 \mu\text{M}$ ) of **1** and **2** were respectively titrated with increasing amounts of CT-DNA. In the absence and presence of CT-DNA, **1** and **2** emit luminescence in *Tris* buffer, with a maximum appearing at 587 nm and 592 nm, respectively. Upon addition of CT-DNA, the emission intensities for **1** and **2** grow to around 2.02 and 2.97 times larger than that in the absence of DNA and saturates at a  $[\text{DNA}]/[\text{Ru}]$  ratio of 25:1. This implies that both complexes strongly interact with



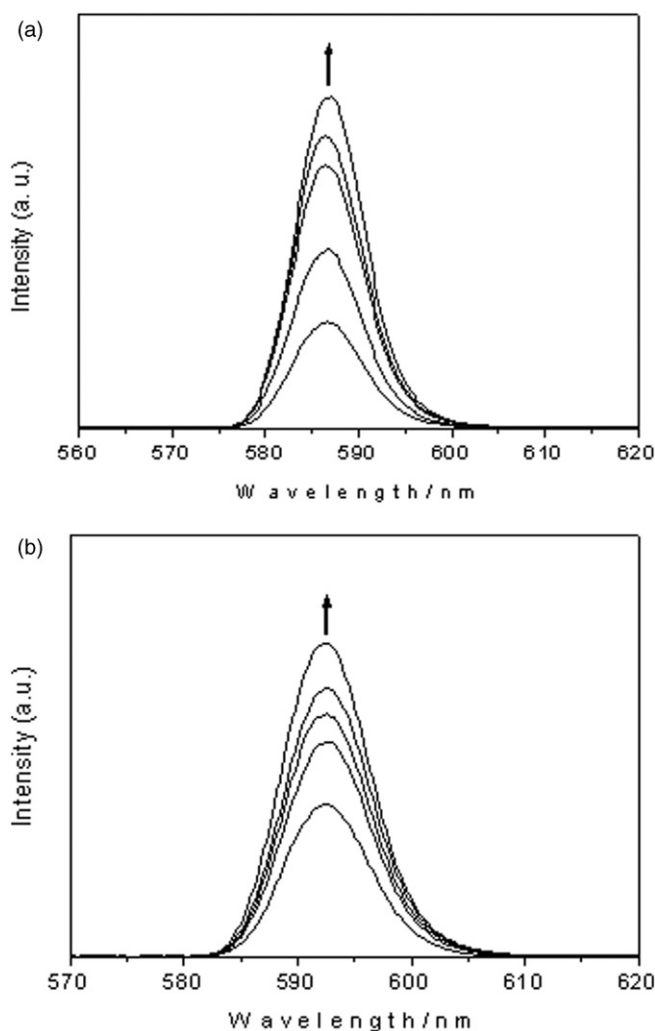


Figure 3. Emission spectra of **1**(a) and **2**(b) in *Tris*-HCl buffer in the absence and presence of CT-DNA. Arrow shows the intensity change upon increasing DNA concentration.

DNA and can be protected by DNA efficiently. The extent of enhancement increases on going from  $[\text{Ru}(\text{dmp})_2(\text{PYNI})]^{2+}$  to  $[\text{Ru}(\text{phen})_2(\text{PYNI})]^{2+}$ , which is consistent with the above absorption spectra results.

Steady-state emission quenching using  $[\text{Fe}(\text{CN})_6]^{4-}$  as quencher is used to observe the binding of  $[\text{Ru}(\text{phen})_2(\text{PYNI})]^{2+}$  and  $[\text{Ru}(\text{dmp})_2(\text{PYNI})]^{2+}$  with CT-DNA. As illustrated in figure 4, in the absence of DNA, the Ru(II) complex is efficiently quenched by  $[\text{Fe}(\text{CN})_6]^{4-}$ , resulting in a linear Stern-Volmer plot with a slope of 2.83 and 2.03 for complexes  $[\text{Ru}(\text{phen})_2(\text{PYNI})]^{2+}$  and  $[\text{Ru}(\text{dmp})_2(\text{PYNI})]^{2+}$ . In the presence of DNA, however, the Stern-Volmer plot changes drastically, and the efficiency of quenching (slope 0.13 and 0.33 for complexes **1** and **2**, respectively) of the Ru(II) complex bound to DNA by  $[\text{Fe}(\text{CN})_6]^{4-}$  decreased relative to that of the free

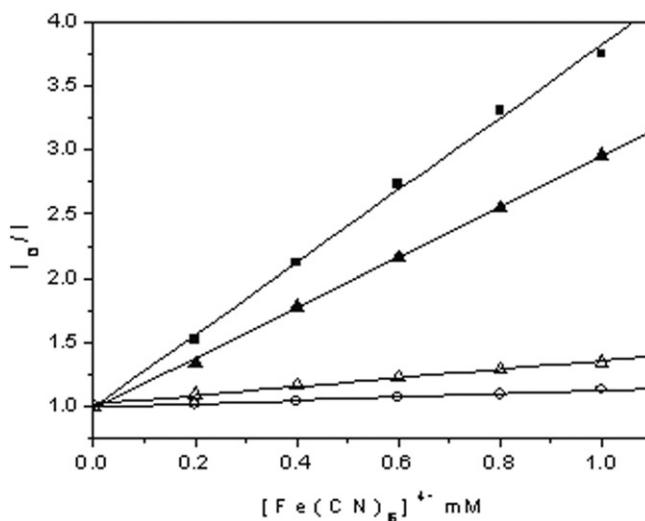


Figure 4. Emission quenching curves of complexes with increasing concentration of quencher  $[\text{Fe}(\text{CN})_6]^{4-}$  in the absence:  $[\text{Ru}(\text{phen})_2(\text{PYNI})]^{2+}$  (■),  $[\text{Ru}(\text{dmp})_2(\text{PYNI})]^{2+}$  (▲) and presence:  $[\text{Ru}(\text{phen})_2(\text{PYNI})]^{2+}$  (○) and  $[\text{Ru}(\text{dmp})_2(\text{PYNI})]^{2+}$  (△) of CT-DNA.  $[\text{Ru}] = 5 \mu\text{M}$ .

Ru(II) complex. This may be explained by the fact that the bound cations of the Ru(II) complex are protected from the anionic water-bound quencher by the negative DNA phosphate backbone, hindering quenching of the emission of bound complexes [48, 49]. The slope can be taken as a measure of binding affinity, a large slope corresponding to poor protection and low binding [48, 49].

### 3.4. Viscosity measurements

In the absence of crystallographic structural data or NMR spectra, viscosity is useful to prove intercalation [50]. Under appropriate conditions, intercalation of drugs like ethidium bromide (EB) causes a significant increase in viscosity of DNA solution due to the increase in separation of base pairs of intercalation sites and hence an increase in overall DNA contour length. On the other hand, drug molecules binding exclusively in the DNA grooves cause less pronounced, or no obvious change, in DNA solution viscosity [51], a partial and/or non-classical intercalation of ligand could bend (or kink) the DNA helix, reduces its effective length and, concomitantly, its viscosity [50, 52]. The effects of the complexes  $[\text{Ru}(\text{phen})_2(\text{PYNI})]^{2+}$ ,  $[\text{Ru}(\text{dmp})_2(\text{PYNI})]^{2+}$  together with  $[\text{Ru}(\text{bpy})_3]^{2+}$  and ethidium bromide (EB) on the viscosity of rod-like DNA are shown in figure 5. Ethidium bromide is a known DNA classical intercalator and increases the relative specific viscosity for lengthening of the DNA double helix through intercalation; while for  $[\text{Ru}(\text{bpy})_3]^{2+}$ , which has been well known to bind with DNA only through electrostatic mode, it exerts essentially no effect on DNA viscosity. On increasing the amounts of **1**, figure 4 indicates the relative viscosity of DNA increases steadily, similar to the behavior of the ethidium bromide. By contrast, on increasing the amount of **2**, the relative viscosity of DNA decreases. The experimental results suggest

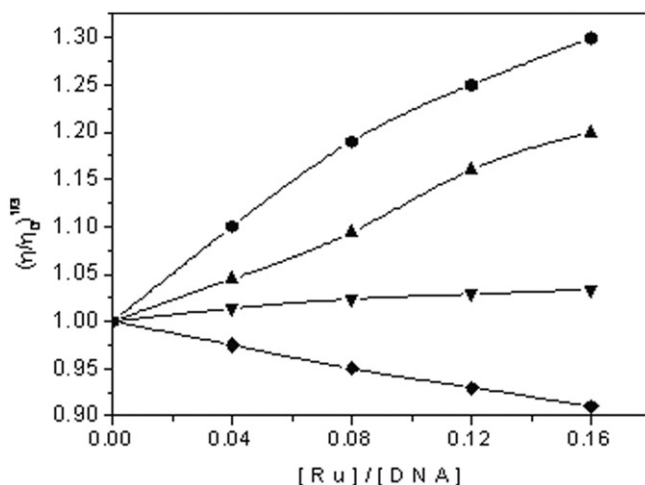


Figure 5. Effect of increasing amounts of EB (●),  $[\text{Ru}(\text{phen})_2(\text{PYNI})]^{2+}$  (▲),  $[\text{Ru}(\text{bpy})_3]^{2+}$  (▼) and  $[\text{Ru}(\text{dmp})_2(\text{PYNI})]^{2+}$  (■) on the relative viscosity of CT-DNA at  $28 (\pm 0.1)^\circ\text{C}$ .  $[\text{DNA}] = 0.5 \text{ mM}$ .

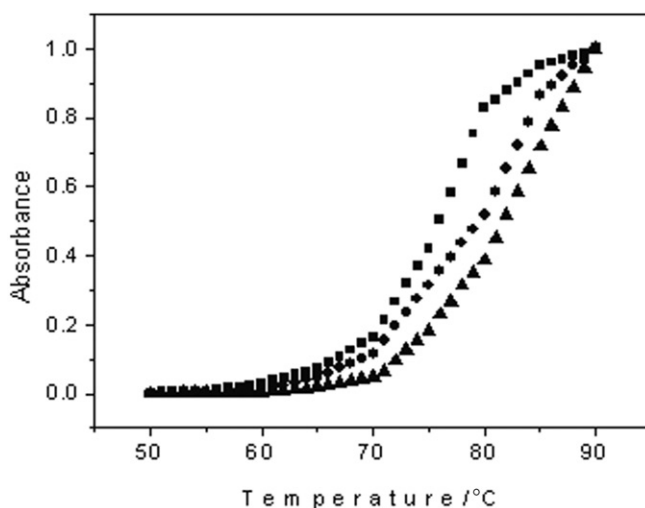


Figure 6. Thermal denaturation of calf thymus DNA in the absence (■) and presence of **1** (▲) and **2** (●),  $[\text{Ru}] = 20 \mu\text{M}$ ,  $[\text{DNA}] = 100 \mu\text{M}$ .

that **1** binds to DNA through a classical intercalation mode, while **2** binds to DNA not by the classical intercalation mode but by the partial, non-classical intercalation model.

### 3.5. Thermal denaturation studies

The melting of DNA can be used to distinguish between molecules which bind via intercalation and those which bind externally, and thermal denaturation behavior of DNA can offer information about the interaction strength of complexes with DNA. Generally, the melting temperature increases when metal complexes bind to DNA by

intercalation, as intercalation of the complexes into DNA base pairs causes stabilization of base stacking and hence raises the melting temperature of the double-stranded DNA; DNA melting experiments are useful in establishing the extent of intercalation [53]. The melting temperature  $T_m$ , which is defined as the temperature where half of the total base pairs are unbound, is determined from the thermal denaturation curves of DNA by monitoring changes of absorption spectra of DNA bases ( $\lambda = 260$  nm). When the temperature in the solution increases, double-stranded DNA gradually dissociates to single strands and generates a hypochromic effect on the absorption spectra of DNA solution. According to the literature [53–55], the intercalation of natural or synthesized organics and metallointercalators generally results in a considerable increase in melting temperature ( $T_m$ ). Here, a DNA melting experiment revealed that  $T_m$  of calf thymus DNA is  $75.3 \pm 0.5^\circ\text{C}$  in the absence of the complexes (figure 6) under our experimental conditions. The observed melting temperature in the presence of **1** and **2** were  $83.0 \pm 0.5^\circ\text{C}$  and  $80.1 \pm 0.5^\circ\text{C}$ , respectively. The large increases in  $T_m$  of **1** ( $\Delta T_m = 7.7^\circ\text{C}$ ) and the moderate increases in  $T_m$  of **2** ( $\Delta T_m = 4.8^\circ\text{C}$ ) are comparable to that observed for classical intercalators [53–55] and lend strong support for intercalation into the helix. The experimental results also indicate that **1** exhibits larger DNA-binding affinity than does **2**.

#### 4. Conclusion

Two new Ru(II) complexes,  $[\text{Ru}(\text{phen})_2(\text{PYNI})]^{2+}$  and  $[\text{Ru}(\text{dmp})_2(\text{PYNI})]^{2+}$ , have been synthesized and characterized. The DNA-binding of the two Ru(II) complexes has been investigated by absorption spectroscopy, luminescence spectroscopy, viscosity measurements and thermal denaturation. The spectroscopic titration and thermal denaturation suggest that the two complexes moderately bind to CT-DNA. Substitution on the 2- and 9-positions of the ancillary phen ligands may cause severe steric constraints near the core of  $\text{Ru}^{\text{II}}$  when the complex intercalates into the DNA base pairs and prevent the complex from intercalating effectively; the DNA-binding affinity for **2** is smaller than that for **1**. Results show that **1** intercalates into the DNA base pairs, while **2** can bind to CT-DNA by partial intercalation.

#### Acknowledgements

We are grateful to the Nature Science Foundation of Guangdong Province (No. 0711220400121) and Guangdong Pharmaceutical University for financial support.

#### References

- [1] K.E. Erkkila, D.T. Odom, J.K. Barton. *Chem. Rev.*, **99**, 2777 (1999).
- [2] C. Metcalfe, J.A. Thomas. *Chem. Soc. Rev.*, **32**, 215 (2003).
- [3] Y. Xiong, L.N. Ji. *Coord. Chem. Rev.*, **185–186**, 711 (1999).
- [4] A. Sigel, H. Sigel (Eds.), *Metal Ions in Biological Systems*, Vol. 33, Marcel Dekker, New York, 177 (1996).

- [5] L.-N. Ji, X.-H. Zou, J.-G. Liu. *Coord. Chem. Rev.*, **216–217**, 513 (2001).
- [6] L.N. Ji, Q.L. Zhang, H. Chao. *Chinese Sci. Bull.*, **46**, 1332 (2001).
- [7] A.E. Friedman, C.V. Kumar, N.J. Turro, J.K. Barton. *Nucleic Acids Res.*, **19**, 2595 (1991).
- [8] J.C. Chambron, J.P. Sauvage, E. Amouyal, P. Koffi. *New J. Chem.*, **9**, 527 (1985).
- [9] Y. Jenkins, A.E. Friedman, N.J. Turro, J.K. Barton. *Biochemistry*, **31**, 10809 (1992).
- [10] A.E. Friedman, J.C. Chambron, J.P. Sauvage, N.J. Turro, J.K. Barton. *J. Am. Chem. Soc.*, **112**, 4960 (1990).
- [11] L. Haq, P. Lincoln, D. Suh, B. Nordén, B.Z. Chowdhry, J.B. Chaires. *J. Am. Chem. Soc.*, **117**, 4788 (1995).
- [12] C. Turro, S.H. Bossmann, Y. Jenkins, J.K. Barton, N.J. Turro. *J. Am. Chem. Soc.*, **117**, 9026 (1995).
- [13] R.B. Nair, B.M. Cullum, C.J. Murphy. *Inorg. Chem.*, **36**, 962 (1997).
- [14] P. Lincoln, A. Broo, B. Nordén. *J. Am. Chem. Soc.*, **118**, 2644 (1996).
- [15] S.D. Choi, M.-S. Kim, S.K. Kim, P. Lincoln, E. Tuite, B. Nordén. *Biochemistry*, **36**, 214 (1997).
- [16] E.D.A. Stemp, M.R. Arkin, J.K. Barton. *J. Am. Chem. Soc.*, **119**, 2921 (1997).
- [17] R.E. Holmlin, E.D.A. Stemp, J.K. Barton. *Inorg. Chem.*, **37**, 29 (1998).
- [18] E. Tuite, P. Lincoln, B. Nordén. *J. Am. Chem. Soc.*, **119**, 239 (1997).
- [19] J.R. Schoonover, W.D. Bates, T.J. Meyer. *Inorg. Chem.*, **34**, 6421 (1995).
- [20] Y. Jenkins, J.K. Barton. *J. Am. Chem. Soc.*, **114**, 8736 (1992).
- [21] C.M. Dupureur, J.K. Barton. *Inorg. Chem.*, **36**, 33 (1997).
- [22] C.M. Dupureur, J.K. Barton. *J. Am. Chem. Soc.*, **116**, 10286 (1994).
- [23] M. Eriksson, M. Leijon, C. Hiort, B. Nordén, A. Graeslund. *Biochemistry*, **33**, 5031 (1994).
- [24] C. Hiort, P. Lincoln, B. Nordén. *J. Am. Chem. Soc.*, **115**, 3448 (1993).
- [25] M.R. Arkin, E.D.A. Stemp, R.E. Holmlin, J.K. Barton, A. Hormann, E.J.C. Olson, P.F. Barbara. *Science*, **273**, 475 (1996).
- [26] A.M. Pyle, J.P. Rehmman, R. Meshoyrer, C.V. Kumar, N.J. Turro, J.K. Barton. *J. Am. Chem. Soc.*, **111**, 3051 (1989).
- [27] J. Marmur. *J. Mol. Biol.*, **3**, 208 (1961).
- [28] M.E. Reichmann, S.A. Rice, C.A. Thomas, P. Doty. *J. Am. Chem. Soc.*, **76**, 3047 (1954).
- [29] A. Wolfe, G.H. Shimer, Jr, T. Meehan. *Biochemistry*, **26**, 6392 (1987).
- [30] J.R. Lakowicz, G. Weber. *Biochemistry*, **12**, 4161 (1973).
- [31] J.B. Chaires, N. Dattagupta, D.M. Crothers. *Biochemistry*, **21**, 3933 (1982).
- [32] G. Cohen, H. Eisenberg. *Biopolymers*, **8**, 45 (1969).
- [33] B.P. Sullivan, D.J. Salmon, T.J. Meyer. *Inorg. Chem.*, **17**, 3334 (1978).
- [34] J.P. Collin, J.P. Sauvage. *Inorg. Chem.*, **25**, 135 (1986).
- [35] Y.J. Liu, H. Chao, L.F. Tan, Y.X. Yuan, W. Wei, L.N. Ji. *J. Inorg. Biochem.*, **99**, 530 (2005).
- [36] B.K. Ghosh, A. Chkravorty. *Coord. Chem. Rev.*, **95**, 239 (1989).
- [37] T. Matsumura-Inoue, H. Tomoro, M. Kasai, T. Tominiga-Morimoto. *J. Electroanal. Chem.*, **95**, 109 (1979).
- [38] M. Haga. *Inorg. Chim. Acta*, **75**, 29 (1983).
- [39] S. Baitalik, U. Flörke, K. Nag. *J. Chem. Soc., Dalton Trans.*, 719 (1999).
- [40] J.-G. Liu, Q.-L. Zhang, X.-F. Shi, L.-N. Ji. *Inorg. Chem.*, **40**, 5045 (2001).
- [41] J.-Z. Wu, B.-H. Ye, L. Wang, L.-N. Ji, J.-Y. Zhou, R.-H. Li, Z.-Y. Zhou. *J. Chem. Soc., Dalton Trans.*, 1395 (1997).
- [42] Q.-X. Zhen, B.-H. Ye, Q.-L. Zhang, J.-G. Liu, H. Li, L.-N. Ji, L. Wang. *J. Inorg. Biochem.*, **76**, 47 (1999).
- [43] X.-H. Zou, B.-H. Ye, H. Li, J.-G. Liu, Y. Xiong, L.-N. Ji. *J. Chem. Soc., Dalton Trans.*, 1423 (1999).
- [44] H. Deng, J. Cai, H. Xu, H. Zhang, L.N. Ji. *J. Chem. Soc., Dalton Trans.*, 325 (2003).
- [45] P. Lincoln, B. Nordén. *J. Phys. Chem. B*, **102**, 9583 (1998).
- [46] H. Xu, K.C. Zheng, H. Deng, L.J. Lin, Q.L. Zhang, L.N. Ji. *New J. Chem.*, **27**, 1255 (2003).
- [47] J.E. Coury, J.R. Anderson, L. McFail-Isom, L.D. Williams, L.A. Bottomley. *J. Am. Chem. Soc.*, **119**, 3792 (1997).
- [48] C.V. Kumar, J.K. Barton, N.J. Turro. *J. Am. Chem. Soc.*, **107**, 5518 (1985).
- [49] J.K. Barton, J.M. Goldberg, C.V. Kumar, N.J. Turro. *J. Am. Chem. Soc.*, **108**, 2081 (1986).
- [50] S. Satyanarayana, J.C. Dabrowiak, J.B. Chaires. *Biochemistry*, **31**, 9319 (1992).
- [51] L.S. Lerman. *J. Mol. Biol.*, **3**, 18 (1961).
- [52] S. Satyanarayana, J.C. Dabrowiak, J.B. Chaires. *Biochemistry*, **32**, 2573 (1993).
- [53] C.V. Kumar, E.H. Asuncion. *J. Am. Chem. Soc.*, **115**, 8547 (1993).
- [54] J.M. Kelly, A.B. Tossi, D.J. McConnell, C. OhUigin. *Nucleic Acids Res.*, **13**, 6017 (1985).
- [55] G.A. Neyhart, N. Grover, S.R. Smith, W.A. Kalsbeck, T.A. Fairley, M. Cory, H.H. Thorp. *J. Am. Chem. Soc.*, **115**, 4423 (1993).